

HI 21cm emission from the sub-damped Lyman- α absorber at $z = 0.0063$ towards PG 1216+069

J. N. Chengalur^{1*}, T. Ghosh², C. J. Salter², N. Kanekar¹, E. Momjian³, B.A. Keeney⁴, J.T. Stocke⁴

¹National Centre for Radio Astrophysics, TIFR, Ganeshkhind, Pune - 411007, India

²NAIC, Arecibo Observatory, HC3 Box 53995, Arecibo, PR 00612

³National Radio Astronomy Observatory, 1003 Lopezville Road, Socorro, NM 87801-0387

⁴Center for Astrophysics and Space Astronomy, Department of Astrophysical and Planetary Sciences, Box 389, University of Colorado, Boulder, CO 80309

20 February 2018

ABSTRACT

We present HI 21cm emission observations of the $z \sim 0.00632$ sub-damped Lyman- α absorber (sub-DLA) towards PG 1216+069 made using the Arecibo Telescope and the Very Large Array (VLA). The Arecibo HI 21cm spectrum corresponds to an HI mass of $\sim 3.2 \times 10^7 M_{\odot}$, two orders of magnitude smaller than that of a typical spiral galaxy. This is surprising since in the local Universe the cross-section for absorption at high HI column densities is expected to be dominated by spirals. The HI 21cm emission detected in the VLA spectral cube has a low signal-to-noise ratio, and represents only half the total flux seen at Arecibo. Emission from three other sources is detected in the VLA observations, with only one of these sources having an optical counterpart. This group of HI sources appears to be part of complex “W”, believed to lie in the background of the Virgo cluster. While several HI cloud complexes have been found in and around the Virgo cluster, it is unclear whether the ram pressure and galaxy harassment processes that are believed to be responsible for the creation of such clouds in a cluster environment are relevant at the location of this cloud complex. The extremely low metallicity of the gas, $\sim 1/40$ -solar, also makes it unlikely that the sub-DLA consists of material that has been stripped from a galaxy. Thus, while our results have significantly improved our understanding of the host of this sub-DLA, the origin of the gas cloud remains a mystery.

Key words: cosmology: observations — galaxies: ISM — galaxies: evolution — galaxies: formation — radio lines: galaxies

1 INTRODUCTION

Much of what we know about the interstellar medium of high redshift galaxies comes from studies of absorption lines seen in the spectra of distant quasars. In this context, the most interesting systems are those with the highest neutral hydrogen (HI) column densities: in the local Universe, such high column density gas is almost invariably associated with galaxies. The highest HI column density systems are also interesting because the bulk of neutral atomic gas at high redshifts is provided by absorbers with HI column densities $\geq 2 \times 10^{20} \text{ cm}^{-2}$, the so-called damped Lyman- α absorbers (DLAs; Wolfe et al. 2005). At these column densities, the gas is predominantly neutral, making DLAs the best known reservoirs for star formation at high redshifts. Absorption systems with slightly lower HI column densities (in the range $10^{19} - 2 \times 10^{20} \text{ cm}^{-2}$, the

“sub-DLAs”) are significantly ionised, but nonetheless contribute a non-trivial fraction of the total neutral gas at high redshifts. Sub-DLAs are also expected to be arise in galaxies (e.g. Péroux et al. 2005), possibly in their outer regions.

Since absorption-selected galaxy samples contain no luminosity bias, studies of such samples provide information on the nature of “typical” galaxies at different redshifts. However, despite over two decades of study, (e.g. Møller & Warren 1993; Prochaska & Wolfe 1997; Haehnelt et al. 1998; Warren et al. 2001; Kulkarni et al. 2010; Fynbo et al. 2010, 2011; Fumagalli et al. 2015), the nature of the host galaxies of DLAs and sub-DLAs remains unclear. On the theoretical front, numerical simulations (e.g. Pontzen et al. 2008; Rahmati & Schaye 2014) find that DLA hosts span a range of halo masses, albeit with a peak at low mass. For example, Rahmati & Schaye (2014) find that most DLAs are associated with low-mass ($\lesssim 10^{10} M_{\odot}$) halos, but that the highest HI column density DLAs arise in more massive galaxies.

Unfortunately, there are very few direct observational con-

* E-mail: chengalu@ncra.tifr.res.in

straints on these theoretical models for the host galaxies of high redshift DLAs. This is because identification of the host galaxies of DLAs at $z \gtrsim 2$ via direct imaging has proved to be extremely difficult, even with the Hubble Space Telescope (HST) or 8m-class ground-based optical telescopes. The faint stellar emission from the foreground galaxy typically lies directly below the bright emission from the background quasar making it very difficult to identify the host. Galaxy counterparts are hence known only for a handful of high- z DLAs, mostly systems with high metallicities (e.g. Fynbo et al. 2010, 2011; Krogager et al. 2012; but see also Noterdaeme et al. 2012). This dynamic range problem can be overcome for sightlines with at least two high column density absorbers – the higher-redshift absorber can be used as a filter to block the quasar radiation, allowing a clean measurement of the stellar emission from the lower redshift system (O’Meara et al. 2006; Fumagalli et al. 2010, 2014). Observations of 32 DLAs using this technique have led to stringent constraints on the star formation rate (SFR) of their host galaxies, with the 2σ SFR limits of $\approx 0.09 - 0.27 M_{\odot}$ per year suggesting that the hosts are small galaxies with low star formation (Fumagalli et al. 2014, 2015). This picture is consistent with both the typical low metallicities of the absorbers (e.g. Pettini et al. 1994; Prochaska et al. 2003; Kulkarni et al. 2005), as well as with their typical high spin temperatures (e.g. Kanekar & Chengalur 2003; Kanekar et al. 2014).

At low redshifts ($z \lesssim 1$), information is now available on the optical luminosity, stellar mass, star formation rate, etc. of about twenty DLAs and sub-DLAs (e.g. le Brun et al. 1997; Rao et al. 2003, 2011; Chen et al. 2005). However, little is known about their gas mass and distribution. This is unfortunate, since the gas distribution is a critical physical parameter in absorption-selected samples. If one extrapolates from the properties of the $z \sim 0$ galaxy population, one would expect the cross-section for DLA absorption, particularly at the high HI column density end, to be dominated by large spiral galaxies (Zwaan et al. 2005; Patra et al. 2013). HI 21cm emission studies of DLAs allow a direct determination of the gas mass, the velocity field, and the size of the gas reservoir of the host system. Unfortunately, the weakness of the HI 21cm transition has meant that such searches have only been possible in a handful of DLAs and sub-DLAs, those at the lowest redshifts, $z \lesssim 0.1$ (Kanekar et al. 2001; Bowen et al. 2001; Chengalur & Kanekar 2002; Kanekar & Chengalur 2005; Mazumdar et al. 2014). To date, good quality HI 21cm imaging is available for only one DLA, at $z = 0.009$ towards SBS 1543+593 (Bowen et al. 2001; Chengalur & Kanekar 2002). A tentative detection of HI 21cm emission has been reported in a sub-DLA at $z = 0.006$ towards PG 1216+069 (Briggs & Barnes 2006; Tripp 2008), and strong upper limits on the HI mass, $\lesssim 3 \times 10^9 M_{\odot}$, have been obtained for three other DLAs and sub-DLAs, all at $z \approx 0.1$ (Kanekar et al. 2001; Mazumdar et al. 2014).

In this paper, we present results from a search for HI 21cm emission from the $z = 0.00632$ sub-DLA towards PG 1216+069. This system was observed using the Space Telescope Imaging Spectrograph (STIS) onboard the HST by Tripp et al. (2005) as part of a large survey for low-redshift OVI absorbers, but was discovered serendipitously to have a damped Ly- α profile. Follow-up HI 21cm emission observations were conducted by a number of authors, with tentative detections of HI 21cm emission reported using the Westerbork Synthesis Radio Telescope (WSRT; Briggs & Barnes 2006) and the Very Large Array (VLA; Tripp 2008). Here, we present results based on observations with the Arecibo 305-m telescope, as well as a re-analysis of the archival VLA data. The Arecibo spectrum has an excellent signal-to-noise

ratio, allowing us to robustly measure the HI content of the galaxy. The VLA data allow us to further constrain the spatial extent of the emitting gas, as well as to study the environment of the host system. The rest of this paper is arranged as follows. Section 2 presents the observations and data reduction, while our results are presented in Section 3 and discussed in Section 4.

2 OBSERVATIONS AND DATA REDUCTION

The Arecibo telescope observations (centred at $RA_{J2000}=12:19:20.88$, $DEC_{J2000}=+06:38:38.4$) of the $z = 0.00632$ sub-DLA towards PG 1216+069 were split into a number of short runs between 2004 December and 2005 April, using the L-Band Wide (LBW) receiver and two orthogonal linear polarisations. Passbands of 12.5 and 25 MHz centred on the redshifted HI 21cm line frequency for $z = 0.00632$ were observed simultaneously, each sub-divided into 2048 frequency channels by the spectrometer. Standard position-switching (ON/OFF) was used for bandpass calibration. For a single scan, both the ON and the OFF phases had a duration of 4 min, with each ON/OFF pair followed by a noise diode calibration of the brightness scale. Spectra were written to disk every 1 sec for subsequent analysis.

The data were analysed using the Arecibo IDL reduction package of Phil Perillat. At the time of the observations, L-band measurements at Arecibo were suffering from a locally generated interference that wandered over the spectrum on a time scale of minutes, contaminating a significant fraction of the data. An IDL subroutine was written to eliminate the worst effects of this interference. This was applied to the data of all scans before the quantity (ON–OFF)/OFF was calculated, and the spectra calibrated into units of $Jy \text{ beam}^{-1}$. The interference excision procedure succeeded in salvaging the vast majority of affected scans, and very few had to be rejected. A weighted average of the individual Hanning-smoothed spectra was then taken and the two polarisations averaged to produce the final spectrum.

After a clear Arecibo detection of HI 21cm emission from the sub-DLA had been obtained, data were acquired using the same ON/OFF mode for four positions offset celestially north, south, east and west by 1.6 arcmin, i.e. roughly half the telescope half-power beamwidth (HPBW), from the position of PG 1216+069. This was done to investigate whether the HI 21cm emission from the sub-DLA (a) was extended, (b) was offset relative to PG 1216+069, or (c) showed kinematical signatures of rotation. These data were analysed in a similar manner to the original data.

The VLA data were obtained in project AT312 (PI: Tripp) on 2005 December 22, when the array was in its ‘D’ configuration (Tripp 2008). The total on-source time was ~ 7 hr. The observations used a bandwidth of 3.125 MHz ($\sim 660 \text{ km s}^{-1}$), divided into 64 spectral channels, giving a channel width of 10.4 km s^{-1} . The integrated HI 21cm emission obtained from these data was earlier presented by Tripp (2008). We re-analysed these data, after downloading them from the VLA archive, using standard procedures in classic AIPS. After initial flux density, gain and bandpass calibration, the visibilities of the target source were separated out for self-calibration. After a single round of phase-only self-calibration, a strong source at the edge of the field of view was subtracted out using the task UVSUB. Following this, the field was imaged again and the brightest detected continuum sources subtracted out again using UVSUB. The field was then imaged once more, and the residual continuum subtracted using the task IMLIN. The continuum emission from the quasar PG 1216+069 itself is fairly weak ($\sim \text{few mJy}$;

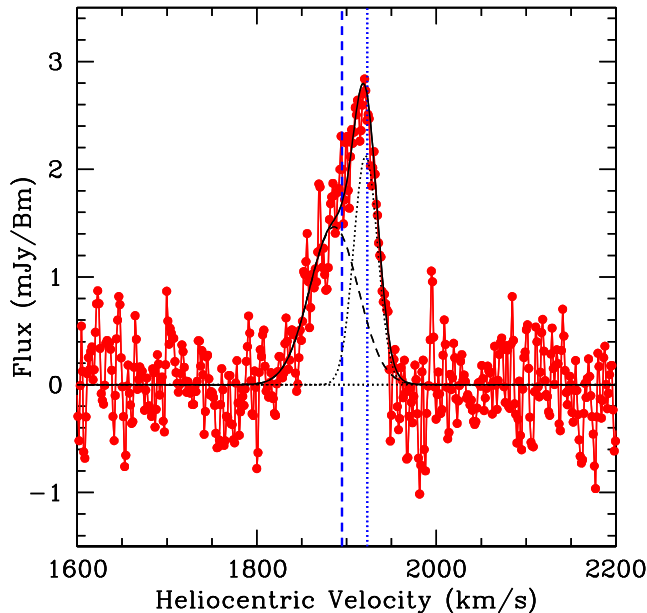


Figure 1. The Arcibo HI 21cm emission spectrum from the $z = 0.00632$ sub-DLA towards PG 1216+069, at a velocity resolution of $\approx 2.6 \text{ km s}^{-1}$. The RMS noise on the spectrum is 0.35 mJy bm^{-1} . The dashed vertical line indicates the redshift measured from the metal lines (viz. $z = 0.00632$), while the dotted line indicates the velocity of the weaker absorption seen in the metal lines by Tripp et al. (2005). The error in the metal line absorption velocity scale is $5 - 10 \text{ km s}^{-1}$ (Tripp et al. 2005). A double Gaussian fit to the Arcibo HI profile is also shown. As can be seen, the velocity of the narrow HI 21cm component matches that of the weaker metal-line absorption.

Kellermann et al. 1989; Kanekar & Chengalur 2005), and does not pose any problems when trying to measure the HI emission along this line of sight. Spectra for all detected objects were finally extracted from the spectral cube, after correcting for the shape of the VLA primary beam, using the task BLSUM.

3 RESULTS

Figure 1 shows the final Arcibo HI 21cm spectrum from the 12.5-MHz passband, at a velocity resolution of $\approx 2.6 \text{ km s}^{-1}$; this is based on 56 min of ON-source data and has a root-mean-square (RMS) noise of 0.35 mJy bm^{-1} . HI 21cm emission from the sub-DLA is detected at the expected redshifted line frequency with a signal-to-noise ratio (S/N) of ≈ 8 per independent channel. The position and velocity of this object indicates that it is a member of cloud “W” which lies in the background of the Virgo cluster (de Vaucouleurs & de Vaucouleurs 1973; Mei et al. 2007), and is believed to be at about twice the Virgo cluster distance (Binggeli et al. 1993). The systemic redshift of $z = 0.00632$ corresponds to a distance of $\approx 28 \text{ Mpc}$ (i.e. approximately twice the distance to the Virgo cluster) in a Lambda cold dark matter (LCDM) cosmology with $H_0 = 68 \text{ km s}^{-1} \text{ Mpc}^{-1}$, $\Omega_M = 0.31$, $\Omega_\Lambda = 0.69$. We use this distance to compute all distance-dependent quantities in this paper. At this assumed distance, the integrated flux density corresponds to an HI mass of $\sim 3.2 \times 10^7 M_\odot$.

The Arcibo HI 21cm spectra from the original and the offset-position observations are shown in Fig. 2. The spectra have been smoothed to a velocity resolution of 24 km s^{-1} to maximise the

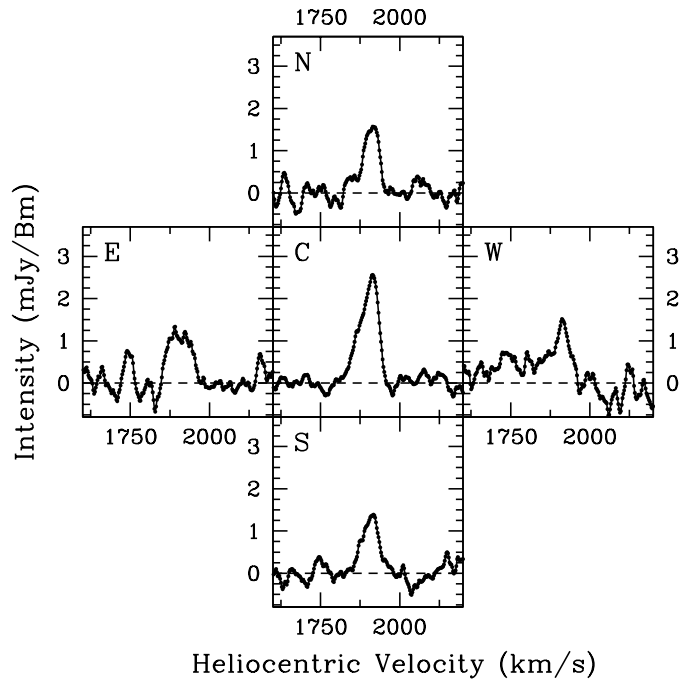


Figure 2. HI 21cm emission spectra derived from the mosaic of pointings around the position of PG 1216+069. The displayed spectra are towards the quasar location, and positions offset to the celestial north, east, south and west by 1.6 arcmin (i.e. \approx half of the telescope HPBW). The observations indicate that the HI 21cm emission detected at Arcibo is unresolved. See the main text for more details.

S/N. At this velocity resolution, the peak S/N at the central location is ≈ 16 per independent velocity channel. The observational and derived parameters for each Arcibo pointing position are presented in Table 1. The columns are (1) the offset direction from PG 1216+069, (2) the ON-source integration time, (3) the RMS noise, (4) the peak HI 21cm flux density, (5) the HI 21cm line integral, in Jy km s^{-1} , (6) the average of the peak HI 21cm intensity and the HI 21cm line integral at an offset position after normalisation by the corresponding values for the central position, (7) the heliocentric radial velocity at peak HI 21cm line intensity, and (8) the velocity width of the HI 21cm line at half power, all at a velocity resolution of 24 km s^{-1} .

HI 21cm emission from four separate sources was detected in the VLA data cube; the integrated HI 21cm emission from these sources is shown in Fig. 3. The cross indicates the position of the background quasar PG 1216+069, while the circles represent the HPBW of the different Arcibo pointings. The position of one of the HI 21cm sources coincides with the quasar location; this source is likely to be the host of the sub-DLA. The derived parameters of the different sources are listed in Table 2, whose columns are (1) the source number, as given in Fig. 3, (2) the central velocity (as estimated from a single-Gaussian fit to the spectral profile), (3) the 50% velocity width (as estimated from the above fit), (4) the integrated HI 21cm flux density (Jy km s^{-1}), and (5) the HI mass of the gas cloud.

4 DISCUSSION

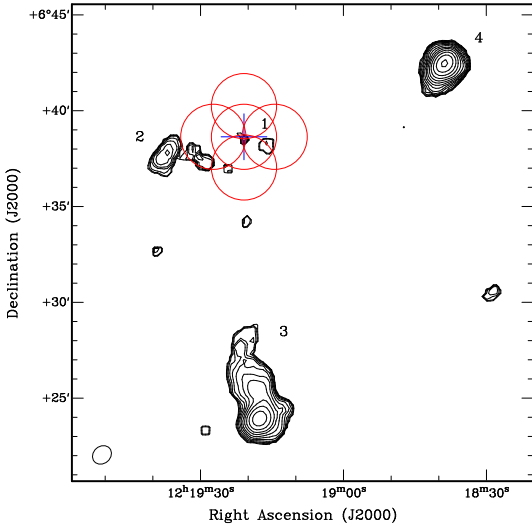
The HI 21cm flux density detected in the central Arcibo pointing can be used to infer the HI mass of the DLA host; this yields an HI

Table 1. Results from the five Arecibo pointings around PG 1216+069.

Posn	T_{int} (min)	RMS noise (mJy bm^{-1})	S_{peak} (mJy bm^{-1})	S_{int} (Jy km s^{-1})	Int_{norm}	V_{peak} km s^{-1}	w_{50} km s^{-1}
Center	56	0.16	2.56	0.1781	–	1914	68
North	36	0.19	1.51	0.1013	0.579	1914	58
South	28	0.20	1.38	0.0901	0.523	1916	64
East	20	0.24	1.12	0.1030	0.508	1905	95
West	16	0.25	1.41	0.0867	0.519	1913	46

Table 2. Parameters of the HI 21cm emission detected in the VLA observations

Source	V_{sys} km s^{-1}	W_{50} km s^{-1}	Integrated Flux density Jy km s^{-1}	HI mass $10^7 M_{\odot}$
1	1907 ± 5	29.5 ± 10.5	0.09 ± 0.02	1.6 ± 0.3
2	1930 ± 16	166.5 ± 38.6	0.38 ± 0.04	6.9 ± 0.9
3	1966 ± 2	45.1 ± 3.8	2.15 ± 0.09	39.7 ± 1.5
4	1990 ± 5	135.5 ± 10.8	1.47 ± 0.06	27.2 ± 1.0

**Figure 3.** The integrated HI 21cm emission detected in the VLA data cube with a resolution of $63'' \times 53''$; the first contour is at an HI column density of $2 \times 10^{18} \text{ cm}^{-2}$, with the HI column density of successive contours increasing in steps of $\sqrt{2}$. The cross marks the location of PG 1216+069, while the circles indicate the HPBW of the Arecibo pointings, resulting in the spectra shown in Figure 2. The four sources detected in the VLA cube are numbered, with numbers increasing anticlockwise about the centre. Source 4 corresponds to the galaxy VCC 297, while the other sources are not associated with any known galaxy.

mass of $\sim 3.2 \times 10^7 M_{\odot}$. As can be seen from Fig. 3, the HPBW of the Arecibo pointing centred on PG 1216+069 includes HI 21cm emission from Source 1 and part of Source 2. Fig. 4 shows the Arecibo HI 21cm spectrum (smoothed to a resolution of 24 km s^{-1}) along with the HI 21cm spectrum derived from the VLA observations. It is apparent that the VLA HI 21cm profile does not contain the tail towards lower velocities that is seen in the Arecibo spectrum. It should be emphasized that Source 2 is at a higher velocity than Source 1 (see Table 2); thus, even if part of the emission from Source 2 contributes to the Arecibo spectrum, it will not reduce the above discrepancy. It thus seems clear that there is some diffuse

HI 21cm emission at lower velocities that is detected at Arecibo, but not at the VLA. A comparison of the flux densities listed in Tables 1 and 2 indicates that about 50% of the flux density detected in the Arecibo HI 21cm spectrum is missing from the VLA profile. In this context, it is worth noting that the HI 21cm emission that we detect for VCC 297 (i.e. Source 4) from the VLA cube is in excellent agreement with that detected in an earlier Arecibo study (Giovanelli et al. 1997), indicating that, in general, the VLA observations are not systematically missing flux.

The results from the multiple Arecibo pointings indicate that the HI 21cm emission detected at Arecibo is well centred on the quasar PG 1216+069. The measured HI 21cm flux densities in the different pointings are consistent with the emitting region being considerably smaller than the Arecibo HPBW ($\approx 3.4'$ at the line frequency of 1410 MHz). For example, a Gaussian emitting region of HPBW $1'$ would only broaden the beam by $\approx 4\%$, while an HPBW of $2'$ would broaden it by $\approx 16\%$. The slightly larger average normalised values of the HI 21cm line intensity in the north-south direction are expected as the Arecibo beam is mildly elliptical (axial ratio ~ 1.15), with the maximum lying along the direction of constant azimuth. Little evidence for systematic rotation can be discerned from the penultimate column of Table 1, implying that the system is either (a) face-on (if disk-like), (b) much smaller than $3.4'$, or (c) has no ordered rotation.

There have been several previous observations that attempted to detect HI 21cm emission from the $z = 0.00632$ sub-DLA. Kanekar & Chengalur (2005) used the Giant Metrewave Radio Telescope (GMRT) to obtain a 5σ limit of $0.06 \text{ Jy km s}^{-1}$ on the integrated HI 21cm flux density (assuming a velocity width of 20 km s^{-1}), thus obtaining the 5σ upper limit of $\sim 1.1 \times 10^7 M_{\odot}$ on the HI mass of the absorber. Later, Briggs & Barnes (2006) used the WSRT to obtain a tentative detection of HI 21cm emission, estimating the HI mass to lie in the range $\sim (0.5 - 1.5) \times 10^7 M_{\odot}$ (consistent with the GMRT non-detection), with a line peak at a velocity of $\sim 1905 \text{ km s}^{-1}$. This is in agreement with the HI 21cm emission detected in our VLA spectrum, for which the measured flux density of Table 2 implies an HI mass of $(1.5 \pm 0.3) \times 10^7 M_{\odot}$. Unfortunately, the WSRT beam is highly elongated at the low declination of the field, making it difficult to determine the morphol-

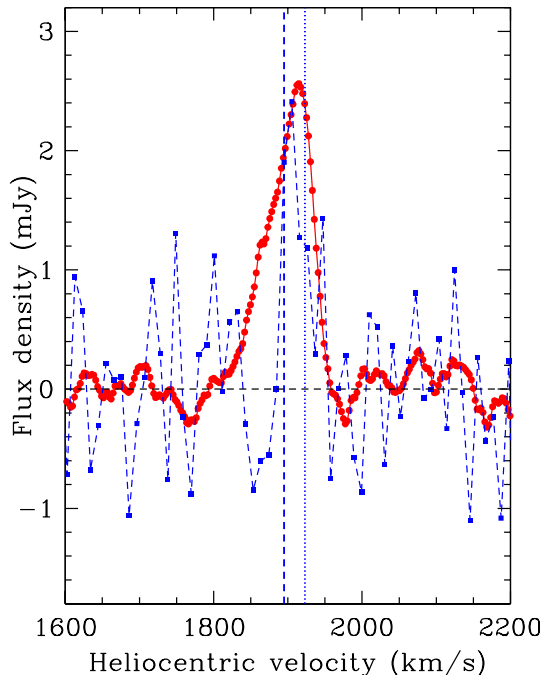


Figure 4. A comparison of the Arecibo HI 21cm spectrum derived from the central pointing towards PG 1216+069 (in solid circles and the solid line) and the HI 21cm spectrum derived from the VLA spectral cube (in solid squares, and the dashed line). The channel spacings of the two spectra are $\approx 24 \text{ km s}^{-1}$ (Arecibo) and $\approx 10.4 \text{ km s}^{-1}$ (VLA). The extended tail of HI 21cm emission seen towards lower velocities at Arecibo does not appear to be detected at the VLA. The dashed vertical line indicates the redshift measured from the metal lines (viz. $z = 0.00632$), while the dotted line indicates the velocity of the weaker absorption seen in the metal lines by Tripp et al. (2005). See the main text for more details.

ogy of the gas associated with the sub-DLA from the WSRT image. However, Briggs & Barnes (2006) note that there is a hint that the HI 21cm emission is extended towards the north-east. Briggs & Barnes (2006) also detected HI 21cm emission from the galaxies VCC 297 and VCC 415 (which lies outside the velocity range covered by the VLA observations), as well as the source labelled 3 in Fig. 3. We note that Tripp (2008) report an HI mass of $\sim 8 \times 10^6 M_{\odot}$ for the host galaxy of the sub-DLA (which corresponds to an HI mass of $\sim 6 \times 10^6 M_{\odot}$ for the distance adopted here). This is smaller (at $\sim 3\sigma$ significance) than our HI mass estimate. Tripp (2008) do not give any details of their data analysis, and the reasons for this discrepancy are unclear.

From Fig. 1, the peak HI 21cm brightness of the sub-DLA is 2.8 mJy bm^{-1} . The heliocentric velocity at the peak HI 21cm intensity is $1917.6 \pm 3.4 \text{ km s}^{-1}$, corresponding to a heliocentric redshift of $z = 0.006396$. The line profile is seen to be asymmetric, extending to lower velocities on the blue side. The line velocity width at half power is $68 \pm 3.4 \text{ km s}^{-1}$, while the velocity width at zero intensity is far wider, $150 \pm 17 \text{ km s}^{-1}$. Interestingly, the weaker component of the low-ionization metal absorption lines detected in the sub-DLA (Tripp et al. 2005) lies at the peak velocity of the HI 21cm emission, while the stronger metal absorption component lies in the extended blue wing of the HI 21cm line. Fig. 1 also shows a two-Gaussian fit to the Arecibo profile. The parameters (amplitude, position and standard deviation) of the Gaussians are $2.1 \pm 0.5 \times 10^{-3} \text{ Jy}$, $1921.2 \pm 1 \text{ km s}^{-1}$, and $13.3 \pm 2 \text{ km s}^{-1}$,

and $1.5 \pm 0.2 \times 10^{-3} \text{ Jy}$, $1885.9 \pm 8 \text{ km s}^{-1}$, and $27.2 \pm 5 \text{ km s}^{-1}$. If we assume that the broad component arises from a diffuse ($\sim 2'$ -sized) cloud, the resulting flux per beam falls below the RMS noise ($\sim 0.4 \text{ mJy}$ for a velocity resolution of $\sim 20 \text{ km s}^{-1}$ and a spatial resolution of $\sim 63''$) of the VLA data cube, consistent with this emission not being detected in the VLA observations.

What is the nature of the HI clouds that give rise to the observed HI 21cm emission? For our assumed distance of 28 Mpc, the absolute blue magnitude of the nearby galaxy VCC 297 is -16.6 mag . (Gavazzi et al. 2006). If the ratio of the HI mass to the blue luminosity in Source 1 is the same as that in VCC 297, one would expect it to have $M_B \sim -13.2 \text{ mag}$, or an apparent magnitude of 18.2 mag. The corresponding numbers for Source 2 and Source 3 are $M_B \sim -15.1 \text{ mag}$ and $M_B \sim -17.0 \text{ mag}$, respectively, or apparent magnitudes of 16.7 mag. and 14.8 mag., respectively. Note that since we are scaling from the values for VCC 297, the apparent magnitudes that we estimate are independent of the assumed distance. Deep optical images of the PG 1216+069 field have been obtained by Prochaska et al. (2011) and Tripp (2008). Unfortunately, the angular resolution of the VLA HI 21cm image is relatively poor, $\approx 1'$, and there are hence multiple optically-identified galaxies within a distance of $0.5'$ of the individual HI clouds. However, none of these galaxies are as bright as the scaled estimates from VCC 297. For example, the brightest objects within $0.5'$ of Sources 2 and 3 have B- and g-magnitudes of ≈ 21.8 (Prochaska et al. 2011) and ≈ 21.0 (SDSS), respectively, $\approx 5 \text{ mag}$. fainter than the scaled estimates from VCC 297. Thus, there appears to be little star formation associated with the neutral gas in Sources 2 and 3. Consistent with this, Gavazzi et al. (2012) do not detect H- α emission from Source 3, obtaining an upper limit of $\text{SFR} < 0.0005 M_{\odot} \text{ yr}^{-1}$. The faintness of the optical counterparts of Sources 2 and 3 thus rules out the possibility that these HI clouds arise in galaxies similar to VCC 297.

In the case of Source 1, its proximity to the background quasar (V magnitude of $\sim 15.4 \text{ mag}$; Hamilton et al. 2008) implies that it would be difficult to detect a faint dwarf galaxy of the above estimated absolute blue magnitude (even with HST imaging of the field; Chen et al. 2001). Indeed, the estimated blue magnitude is similar to that measured for the post-starburst dwarf galaxy J1229+02 (Stocke et al. 2004) that has been suggested to be associated with the metal absorption seen at a heliocentric velocity of 1585 km s^{-1} towards 3C273. This system also lies in the outskirts of the Virgo cluster and the galaxy itself appears to be at an intermediate stage in the fading dwarf evolutionary sequence proposed by Babul & Rees (1992). Keeney et al. (2014) suggest that the observed metal-line absorption system arises from galactic winds from this galaxy interacting with ambient material.

The dynamical mass of the sub-DLA can be estimated as $M_{\text{dyn}} \sim (\Delta V^2 \times R)/G$, where ΔV is the characteristic velocity and R , the characteristic size. If we take ΔV to be half of the FWHM, i.e. $\sim 34 \text{ km s}^{-1}$, and $2R$ to correspond to $\sim 2'$, i.e. intermediate between the VLA and the Arecibo resolutions, the dynamical mass is $\sim 10^9 M_{\odot}$, significantly larger than the estimated HI mass of $3.2 \times 10^7 M_{\odot}$. Conversely, if we assume the size to be that of the VLA resolution of $\sim 1'$ then the dynamical mass would be $\sim 5 \times 10^8 M_{\odot}$. Interestingly, if the size of the sub-DLA is indeed $\sim 2'$, our measured HI mass corresponds to an average HI column density of $\log(N_{\text{HI}}/\text{cm}^{-2}) = 19.29$, very close to the measured value of 19.32 along the quasar sightline (Tripp et al. 2005). If this is indeed the typical HI column density of the system, then it is not surprising that there is no associated star formation.

Tripp et al. (2005) measured an extremely low metallicity, $[O/H] = -1.60^{+0.09}_{-0.11}$, for the $z = 0.00632$ sub-DLA, from the $O\text{I}\lambda 1302$ line, with similar values obtained from multiple SiII lines. Their detection of the FeII lines showed no evidence for the depletion of iron, indicating that the absorber contains very little dust. They also found nitrogen to be under-abundant in the sub-DLA, indicating that the absorber is a primitive, chemically-young galaxy (Tripp et al. 2005). A preliminary analysis of a new HST *Cosmic Origins Spectrograph* ultraviolet spectrum of PG 1216+069 (with a higher S/N ratio than that of the HST-STIS spectrum of Tripp et al. 2005) confirms both the very low metallicity and the underabundance of nitrogen reported by Tripp et al. (2005).

While the HI mass obtained for the sub-DLA towards PG 1216+069 is typical of faint dwarfs, its very low metallicity, $\sim 1/40$ solar (Tripp et al. 2005), is very unusual in the local Universe. From the mass-metallicity relation for dwarf galaxies (Lee et al. 2006), the expected stellar mass for a dwarf galaxy with this metallicity is $\sim 5.4 \times 10^4 M_{\odot}$, i.e. nearly 3 orders of magnitude lower than the HI mass inferred from our Arecibo spectrum. However, we note that there are a few extreme dwarf galaxies which deviate significantly from the mass-metallicity relation at the low-metallicity end (e.g. Ekta & Chengalur 2010). For example, SBS0335-052W has a metallicity of $\sim 1/35$ solar and an HI mass of $5.8 \times 10^8 M_{\odot}$ (Izotov et al. 2005; Ekta et al. 2009). Further, most of the metallicity measurements available in the literature refer to star-forming regions in the centres of dwarf galaxies. Some dwarf irregular galaxies do appear to have significant metallicity gradients (e.g. Pilyugin et al. 2015), and it is possible that gas stripped from the outer parts of such dwarfs could have a low metallicity.

The velocity spread and asymmetry of the HI 21cm emission are both interesting in terms of interpreting the nature of the host galaxy. Fig. 5 shows a plot of W_{50} versus M_{HI} for galaxies from the Local Volume catalogue of Karachentsev et al. (2004). At $M_{\text{HI}} = 3.2 \times 10^7 M_{\odot}$, a velocity width of W_{50} of $\sim 68 \text{ km s}^{-1}$ appears reasonable. However, the highly asymmetric HI 21cm line profile and the large ($\sim 150 \text{ km s}^{-1}$) velocity separation between nulls are both very unusual for a dwarf galaxy (e.g. Begum et al. 2008). Similarly, the presence of significant amounts of diffuse gas (as evidenced by the discrepancy between the VLA and Arecibo HI 21cm flux densities) is unusual for a dwarf galaxy. Thus, although we cannot definitively rule out the possibility that Source 1 is a dwarf galaxy, the available evidence suggests that, like Sources 2 and 3, it too is a hydrogen cloud with very little associated star formation.

Several such “dark” (and “almost dark”; Cannon et al. 2015) HI clouds are known near the Virgo cluster, including HI 1225+01 (Giovanelli & Haynes 1989; Chengalur et al. 1995), Virgo HI21 (Minchin et al. 2005, 2007), and several objects discovered as part of the ALFALFA survey (Kent et al. 2007). The origin of these clouds is as yet unclear. For example, in the case of Virgo HI21, which has an HI mass of $\sim 10^8 M_{\odot}$, the proposed origins include (1) a dark galaxy (Minchin et al. 2005), and (2) a part of a long ($\sim 250 \text{ kpc}$) HI tail stripped from NGC 4254 as it falls at high speed into the Virgo cluster (Haynes et al. 2007). However, the field under study here is further unusual in that it contains 4 HI sources, of which 3 have no optical counterpart. Similarly, Janowiecki et al. (2015) discuss a system of three objects (once again lying behind the Virgo cluster), where only the object with the highest HI flux has an optical counterpart. The origin of the other two HI clouds is unclear. The Virgo cluster appears to be a rich hunting ground for such small groups of clouds: Kent et al. (2009) discuss a field in which there are 5 HI clouds. Interferometric studies of the HI

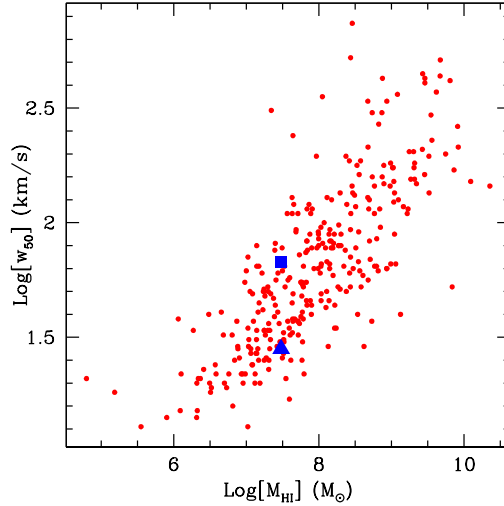


Figure 5. The velocity width between 50% points (W_{50}) plotted versus HI mass for the galaxies in the Karachentsev et al. (2004) sample. With an HI mass of $\sim 3.2 \times 10^7 M_{\odot}$ and $W_{50} \sim 68 \text{ km s}^{-1}$, the properties of Source-1 (indicated by the solid square) are not significantly discrepant from those of the galaxies in this sample. The solid triangle marks the same HI mass, but the velocity width is taken to be 28 km s^{-1} , corresponding to the velocity separation between the two metal-line absorption systems associated with this system (Tripp et al. 2005). See the main text for more details.

clouds in the Virgo cluster have clearly identified some of these objects as debris from larger galaxies, but the origin of several other clouds remains unclear (e.g. Kent et al. 2009; Kent 2010). Kent et al. (2009) present a model in which the clouds have been stripped from a larger galaxy on its first passage through the intra-cluster medium (ICM), estimating the evaporation timescale (due to interactions with the hot ICM) for such clouds to be very short, $\lesssim 10^8 \text{ yr}$. They find that such clouds could be present at distances as large as $\approx 240 \text{ kpc}$ from the parent galaxy. Other studies have also demonstrated the importance of ram pressure stripping of galaxies falling into the Virgo cluster. For example, NGC 4388 has a $\sim 100 \text{ kpc}$ -long tail that is believed to have been produced by ram pressure stripping (Oosterloo & van Gorkom 2005). Chung et al. (2007) find that several of the spiral galaxies with projected separations of $< 1 \text{ Mpc}$ from M87 have HI tails pointing away from M87, again indicative of gas stripping due to ram pressure. In this context, it is interesting to note that both Sources 2 and 3 are extended in the north-south direction (i.e. roughly radially from M87). Fig. 6 shows a higher resolution VLA image of the integrated HI 21cm emission of VCC297; the extension of the emission in the north-south direction is again quite clear. Unfortunately, at this resolution, no emission from Sources 1 and 2 is detected, and only the dense clump of Source 3 is seen. The fact that the majority of the sources detected in this field are extended along the direction towards M87 suggests that these gas clouds may be debris left behind due to ram-pressure stripping of a small group of galaxies that is falling into the Virgo cluster. The total mass of the clouds that we detect (i.e. Sources 1, 2 and 3) is $\sim \text{few} \times 10^8 M_{\odot}$, similar to the total mass of the cloud complex studied by Kent et al. (2009). As discussed in Briggs & Barnes (2006), there are at least 6 known galaxies within 400 km s^{-1} of Source 1 located in a square region of size $\approx 300 \text{ kpc}$ around the source. In principle, any of these galaxies could be the source of the clouds that we detect in the VLA image. However, the entire cloud complex is located $\gtrsim 2 \text{ Mpc}$ in projec-

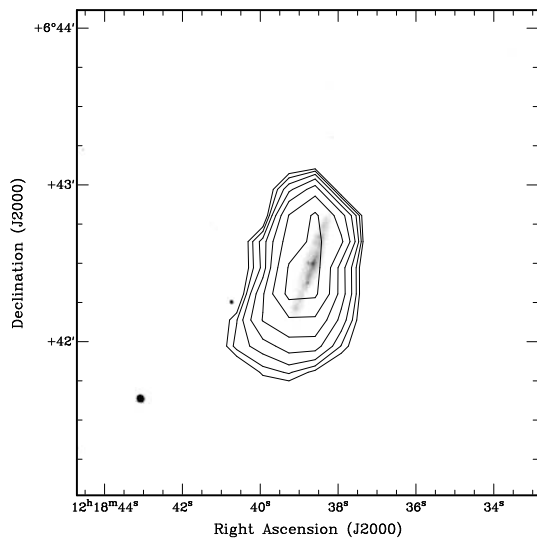


Figure 6. A higher resolution ($39'' \times 39''$) VLA image of the HI 21cm emission from VCC297 (contours) overlaid on the Sloan Digital Sky Survey (SDSS) g-band image (greyscale). The HI 21cm contours start at 2×10^{19} atoms cm^{-2} and increase in steps of $\sqrt{2}$. The HI 21cm emission appears to be extended towards the southern side of the galaxy, possibly because of ram pressure from the surrounding medium. Two of the other sources in this field (Sources 2 and 3; see Fig. 3) also appear to be extended in the north-south direction.

tion away from M87 (although it does lie projected on the outskirts of the X-ray emission around M49; Böhringer et al. 1994) and, if we assume it to be part of complex “W” at twice the Virgo distance, it is unclear whether the ram pressure at this location would be sufficient to strip the gas from the parent galaxy. Further, even for the sources that are extended in the north-south direction, the tails themselves point in different directions. An even more serious consideration is the extremely low metallicity of the gas detected in absorption in Source 1. As discussed above, there are very few known galaxies in the local Universe with such low metallicities; it hence appears unlikely that this gas arises from the stripping of the interstellar medium of a normal galaxy. Thus, although the currently available observations have significantly advanced our understanding of the host of the $z = 0.00632$ sub-DLA, they also raise several further puzzles.

5 SUMMARY

We present the results of Arecibo observations of HI 21cm emission from the $z \sim 0.00632$ sub-DLA seen towards the quasar PG 1216+069. HI 21cm emission is clearly detected at Arecibo, yielding an HI mass of $\sim 3.2 \times 10^7 M_{\odot}$. From a mosaic of pointings around the quasar location, we find that the HI 21cm emission is not extended in comparison to the Arecibo angular resolution of $\sim 3.4'$. The offset pointings also show no evidence for a systematic velocity gradient in the HI 21cm emission.

Our analysis of archival VLA data on this source also yields a detection of HI 21cm emission in images with an angular resolution of $\sim 63''$. However, the VLA images recover only about 50% of the flux detected at Arecibo. We also detect HI 21cm emission from 3 other sources in the same field of view, only one of which is associated with a known optically-detected galaxy. We find the HI 21cm emission from all of the sources, except that which hosts

the sub-DLA (for which the S/N is very low), to be extended in the north-south direction, although the emission tails are themselves not aligned. The entire complex appears to be part of complex “W” that is believed to be behind the Virgo cluster, and at about twice its distance. It is unclear whether the gas stripping mechanisms that operate in clusters are relevant at the large distance ($\gtrsim 2$ Mpc) of this complex from Virgo. Further, the extremely low metallicity of the sub-DLA ($\sim 1/40$ solar) makes it unlikely that this material has been stripped from a normal galaxy; there are only a handful of galaxies with such low metallicities in the local Universe. In summary, while the $z \sim 0.006$ absorber towards PG 1216+69 is one of only two known DLAs or sub-DLAs with detected HI 21cm emission, providing an estimate of its total gas mass, there are several unresolved puzzles about the origin of this system.

6 ACKNOWLEDGMENTS

The Arecibo Observatory is operated by SRI International under a cooperative agreement with the National Science Foundation (AST-1100968), and in alliance with Ana G. Méndez-Universidad Metropolitana, and the Universities Space Research Association. The National Radio Astronomy Observatory is a facility of the National Science Foundation, operated under cooperative agreement by Associated Universities, Inc. NK acknowledges support from the DST, India, via a Swarnajayanti Fellowship. We are grateful to the anonymous referee for comments which have led to improvements in the paper.

REFERENCES

- Babul A., Rees M. J., 1992, *MNRAS*, 255, 346
- Begum A., Chengalur J. N., Karachentsev I. D., Sharina M. E., Kaisin S. S., 2008, *MNRAS*, 386, 1667
- Binggeli B., Popescu C. C., Tammann G. A., 1993, *A&AS*, 98, 275
- Böhringer H., Briel U. G., Schwarz R. A., Voges W., Hartner G., Trümper J., 1994, *Nature*, 368, 828
- Bowen D. V., Huchtmeier W., Brinks E., Tripp T. M., Jenkins E. B., 2001, *A&A*, 372, 820
- Briggs F. H., Barnes D. G., 2006, *ApJ*, 640, L127
- Cannon J. M. et al., 2015, *AJ*, 149, 72
- Chen H.-W., Kennicutt Jr. R. C., Rauch M., 2005, *ApJ*, 620, 703
- Chen H.-W., Lanzetta K. M., Webb J. K., Barcons X., 2001, *ApJ*, 559, 654
- Chengalur J. N., Giovanelli R., Haynes M. P., 1995, *AJ*, 109, 2415
- Chengalur J. N., Kanekar N., 2002, *A&A*, 388, 383
- Chung A., van Gorkom J. H., Kenney J. D. P., Vollmer B., 2007, *ApJ*, 659, L115
- de Vaucouleurs G., de Vaucouleurs A., 1973, *A&A*, 28, 109
- Ekta B., Chengalur J. N., 2010, *MNRAS*, 406, 1238
- Ekta B., Pustilnik S. A., Chengalur J. N., 2009, *MNRAS*, 397, 963
- Fumagalli M., O’Meara J. M., Prochaska J. X., Kanekar N., 2010, *MNRAS*, 408, 362
- Fumagalli M., O’Meara J. M., Prochaska J. X., Kanekar N., Wolfe A. M., 2014, *MNRAS*, 444, 1282
- Fumagalli M., O’Meara J. M., Prochaska J. X., Rafelski M., Kanekar N., 2015, *MNRAS*, 446, 3178
- Fynbo J. P. U. et al., 2010, *MNRAS*, 408, 2128
- Fynbo J. P. U. et al., 2011, *MNRAS*, 413, 2481

- Gavazzi G., Boselli A., Cortese L., Arosio I., Gallazzi A., Pedotti P., Carrasco L., 2006, *A&A*, 446, 839
- Gavazzi G., Fumagalli M., Galardo V., Grossetti F., Boselli A., Giovanelli R., Haynes M. P., Fabello S., 2012, *A&A*, 545, 16
- Giovanelli R., Avera E., Karachentsev I. D., 1997, *AJ*, 114, 122
- Giovanelli R., Haynes M. P., 1989, *ApJL*, 346, L5
- Haehnelt M. G., Steinmetz M., Rauch M., 1998, *ApJ*, 495, 64
- Hamilton T. S., Casertano S., Turnshek D. A., 2008, *ApJ*, 678, 22
- Haynes M. P., Giovanelli R., Kent B. R., 2007, *ApJL*, 665, L19
- Izotov Y. I., Thuan T. X., Guseva N. G., 2005, *ApJ*, 632, 210
- Janowiecki S. et al., 2015, *ApJ*, 801, 96
- Kanekar N., Chengalur J. N., 2003, *A&A*, 399, 857
- Kanekar N., Chengalur J. N., 2005, *A&A*, 429, L51
- Kanekar N., Chengalur J. N., Subrahmanyan R., Petitjean P., 2001, *A&A*, 367, 46
- Kanekar N. et al., 2014, *MNRAS*, 438, 2131
- Karachentsev I. D., Karachentseva V. E., Huchtmeier W. K., Makarov D. I., 2004, *AJ*, 127, 2031
- Keeney B. A., Joeris P., Stocke J. T., Danforth C. W., Levesque E. M., 2014, *AJ*, 148, 103
- Kellermann K. I., Sramek R., Schmidt M., Shaffer D. B., Green R., 1989, *AJ*, 98, 1195
- Kent B. R., 2010, *ApJ*, 725, 2333
- Kent B. R. et al., 2007, *ApJL*, 665, L15
- Kent B. R., Spekkens K., Giovanelli R., Haynes M. P., Momjian E., Cortés J. R., Hardy E., West A. A., 2009, *ApJ*, 691, 1595
- Krogager J.-K., Fynbo J. P. U., Møller P., Ledoux C., Noterdaeme P., Christensen L., Milvang-Jensen B., Sparre M., 2012, *MNRAS*, 424, L1
- Kulkarni V. P., Fall S. M., Lauroesch J. T., York D. G., Welty D. E., Khare P., Truran J. W., 2005, *ApJ*, 618, 68
- Kulkarni V. P., Khare P., Som D., Meiring J., York D. G., Péroux C., Lauroesch J. T., 2010, *New Astronomy*, 15, 735
- le Brun V., Bergeron J., Boissé P., Deharveng J.-M., 1997, *A&A*, 321, 733
- Lee H., Skillman E. D., Cannon J. M., Jackson D. C., Gehrz R. D., Polomski E. F., Woodward C. E., 2006, *ApJ*, 647, 970
- Mazumdar P., Kanekar N., Prochaska J. X., 2014, *MNRAS*, 443, L29
- Mei S. et al., 2007, *ApJ*, 655, 144
- Minchin R. et al., 2005, *ApJL*, 622, L21
- Minchin R. et al., 2007, *ApJ*, 670, 1056
- Møller P., Warren S. J., 1993, *A&A*, 270, 43
- Noterdaeme P. et al., 2012, *A&A*, 540, 63
- O'Meara J. M., Chen H.-W., Kaplan D. L., 2006, *ApJL*, 642, L9
- Oosterloo T., van Gorkom J., 2005, *A&A*, 437, L19
- Patra N. N., Chengalur J. N., Begum A., 2013, *MNRAS*, 429, 1596
- Péroux C., Dessauges-Zavadsky M., D'Odorico S., Sun Kim T., McMahon R. G., 2005, *MNRAS*, 363, 479
- Pettini M., Smith L. J., Hunstead R. W., King D. L., 1994, *ApJ*, 426, 79
- Pilyugin L. S., Grebel E. K., Zinchenko I. A., 2015, *MNRAS*, 450, 3254
- Pontzen A. et al., 2008, *MNRAS*, 390, 1349
- Prochaska J. X., Gawiser E., Wolfe A. M., Castro S., Djorgovski S. G., 2003, *ApJL*, 595, L9
- Prochaska J. X., Weiner B., Chen H.-W., Cooksey K. L., Mulchaey J. S., 2011, *ApJS*, 193, 28
- Prochaska J. X., Wolfe A. M., 1997, *ApJ*, 487, 73
- Rahmati A., Schaye J., 2014, *MNRAS*, 438, 529
- Rao S. M., Belfort-Mihalyi M., Turnshek D. A., Monier E. M., Nestor D. B., Quider A., 2011, *MNRAS*, 416, 1215
- Rao S. M., Nestor D. B., Turnshek D. A., Lane W. M., Monier E. M., Bergeron J., 2003, *ApJ*, 595, 94
- Stocke J. T., Keeney B. A., McLin K. M., Rosenberg J. L., Weymann R. J., Giroux M. L., 2004, *ApJ*, 609, 94
- Tripp T. M., 2008, in Minchin R., Momjian E., eds, *The evolution of galaxies through the neutral hydrogen window Vol. 1035 of AIP Conf. Ser., The Synergy of Ultraviolet QSO Absorption Spectroscopy and 21cm Emission Studies*. p. 63
- Tripp T. M., Jenkins E. B., Bowen D. V., Prochaska J. X., Aracil B., Ganguly R., 2005, *ApJ*, 619, 714
- Warren S. J., Møller P., Fall S. M., Jakobsen P., 2001, *MNRAS*, 326, 759
- Wolfe A. M., Gawiser E., Prochaska J. X., 2005, *ARA&A*, 43, 861
- Zwaan M. A., van der Hulst J. M., Briggs F. H., Verheijen M. A. W., Ryan-Weber E. V., 2005, *MNRAS*, 364, 1467